RSC Advances

PAPER

View Article Online
View Journal | View Issue

Cite this: *RSC Adv.*, 2014, **4**, 11919

Online monodisperse droplets based liquid–liquid extraction on a continuously flowing system by using microfluidic devices†

Niejun Wang,‡ Sifeng Mao,‡ Wu Liu, Jing Wu, Haifang Li* and Jin-Ming Lin*

Received 4th February 2014
Accepted 14th February 2014

DOI: 10.1039/c4ra00984c

www.rsc.org/advances

In this work, we developed a chip-based continuously flowing system for online liquid–liquid extraction by using monodisperse droplets, and the droplets containing target compounds after extraction were collected on the microchip. Monodisperse droplets of extracting reagent were on-chip generated and dispersed in continuously flowing sample solution, and then liquid–liquid extraction happened when organic droplets moved forward with sample solution flow. After liquid–liquid extraction, guiding tracks were designed in our system to capture the organic droplets, which allowed the aqueous solution flowing over at the same time. Structures of the microchip were optimized to achieve generation and collection of monodisperse droplets more efficiently. To verify the feasibility of droplet based liquid–liquid extraction on the established platform, we used aqueous solution containing 10 μM fluorescein sodium as sample solution and butanol as the extracting reagent to perform the whole procedures. Fluorescein sodium was successfully extracted by the butanol droplets, and the butanol droplets were successfully collected. The results demonstrated that the developed microfluidic device was a useful tool for monodisperse droplet based liquid–liquid extraction. As all the procedures including droplet generation, extraction and collection were performed on one chip, the established platform had the potential of time-resolved monitoring.

Introduction

Microfluidic device, an outstanding instrument with great potential in many fields,[1–4] has integrated many different kinds of functions such as sample pretreatment, mixing, chemical or biological reactions,[5–9] separation for compounds[10–12] or cells,[13–17] purification and detection. Among those functions, sample pretreatment on microchips is a very important subject. For many situations,[18–20] complex samples will be involved in microfluidic devices and pretreatment of these samples before their further utilization or detection is imperative. Online method for the sample pretreatment also ensures the integration, automation and miniaturization of the functional microfluidic device.

As one of the feasible methods to purify samples on microchip, solid phase extraction (SPE) need immobilization of extracting materials in microchannels,[21–23] which make the fabrication of microchips much more complicated. Meanwhile, multiple procedures including loading, washing and elution are needed during the process of SPE that impedes the real-time or online pretreatment of sample. Compare to SPE, liquid–liquid extraction based on microchip shows excellent advantages.[24,25] Simple introduction of extracting reagent into microchip, which is crucial to achieve the liquid–liquid extraction, can avoid complicated procedures as SPE does and make liquid–liquid extraction well compatible to the flowing system of microfluidic device.

To implement liquid–liquid extraction in microfluidic device, both laminar flow[10] and droplets[26–28] can be utilized and extraction will take place near the liquid–liquid interface. Laminar of sample solution and extracting reagent is usually performed in some microfluidic systems to achieve extraction, while droplets of extracting reagent are introduced into sample solutions in other systems. When similar conditions are applied, droplet-based extraction is more efficient than the stratified one.[29] Several new methods implementing liquid–liquid extraction use captured droplets[28,30] which cannot be released and renewed, so these methods fail to function well in a long-time monitoring or a time-resolved detection. Therefore, developing new methods that are suitable for online time-resolved monitoring will make a great contribution to the development and application of microfluidic devices.

For the successful integration of liquid–liquid extraction onto microfluidic device, sufficient control of the fluid[31] is

Beijing Key Laboratory of Microanalytical Methods and Instrumentation, Department of Chemistry, Tsinghua University, Beijing 100084, China. E-mail: jmlin@mail.tsinghua.edu.cn; lihaifang@mail.tsinghua.edu.cn; Fax: +86 10 62792343; Tel: +86 10 62792343

† Electronic supplementary information (ESI) available: Additional information as noted in text. See DOI: 10.1039/c4ra00984c

‡ These authors contributed equally to this work.

always necessary. In order to develop some novel methods for online time-resolved monitoring, it is urgent to design ingenious methods for the control of fluid. Generation[32,33] and control of droplets,[34–36] two of the important fundamental subjects on microfluidic device, are widely studied and utilized. In the reported methods, T-junction[32,37] and flow focusing[33,38] are the most common ways to generate droplets on microchip, and these droplets can be captured or manipulated. Besides, plug-liked droplets[26,27,39] and monodisperse droplets[40] can also be generated on microchip. Comparing to plug-like droplets in microchannels, monodisperse droplets increase the specific surface area, which enhances the exchange of substance between droplets and continuous phase. So monodisperse droplets show better properties than the other types of droplets. But the collection and recycle of monodisperse droplets remain to be a challenge because monodisperse droplets usually float in continuous phase randomly, which limit the application of monodisperse droplets in extraction in a continuous flowing system. A suitable method to collection these monodisperse droplets will promote the application of monodisperse droplets in microfluidic devices.

In this paper, we developed a novel method for online liquid–liquid extraction on microfluidic device using monodisperse droplets and these monodisperse droplets were collected from a continuously flowing system successfully using guiding tracks. Monodisperse droplets of extracting reagent were firstly generated on microchip and dispersed in the continuously flowing sample solution to simulate the emulsification in traditional liquid–liquid extraction. At the interface between the monodisperse droplets and the sample flow, fast extraction was achieved while the droplets moved forward with the sample solution. Then these droplets were collected by guiding tracks and detected. To confirm the effectiveness of online rapid extraction in this system, fluorescent dye was chosen as model molecules because of the excellent transparency of the microchips which made fluorescence microscope to be a convenient tool to record time-resolved and spatial-resolved signals. Moreover, those collected droplets could be guided to downstream devices for further detection and analysis. As the monodisperse droplets were continuously generated and collected, the extracting reagent kept renewing as time passed, which made this method potential for online time-resolved monitoring.

Experimental

Microdevice design and fabrication

The mould of microchip was fabricated by standard soft lithography method.[41] A silicon wafer was boiled in the mixture of H_2SO_4 and H_2O_2 at a ratio of 3 : 1 (v/v) for 40 min. After washing and drying off, a layer of 50 μm SU-8 photoresist (Microchem, Newton, CA) was coated on the silicon wafer using a spin coater. Then the wafer was pre-baked in 65 °C for 1 min and then in 95 °C for 2 min. The wafer was exposed to UV light through a mask to copy the patterns of the mask onto the wafer. After post baking (65 °C for 1 min and then 95 °C for 2 min), the first layer of the microchip had been copied onto the wafer. For the second and the third exposure, similar procedures were carried out to copy the second layer and the third layer of microchip onto the wafer. With multiple layers of patterns copied onto the wafer, mould of microchips that had difference in height could be acquired. After all the patterns had been copied onto the wafer, development was carried out to wash away the unpolymerized SU-8 photoresist. Silanization was also needed to get the final mould of the microchips. After that, prepolymer of poly(dimethylsiloxane) (PDMS, Sylgard 184, Dow corning, Midland, MI) was mixed with its initiator in a weight ratio of 10 : 1. After the mixture was poured onto the mould and degassed, the mould was baked in 75 °C for 2 h to allow the sufficient polymerization of PDMS. Then PDMS was peeled off from the mould and holes for inlets or outlets were punched. After oxygen plasma treatment, the PDMS was sealed with a cleaned glass slide and then placed in the oven at 75 °C.

According to the proposed function of this platform, three functional sections were designed to perform monodisperse droplets liquid–liquid extraction (Fig. 1): droplets generation part, liquid–liquid extraction part and droplets collection part. In droplets generation part (Fig. 1a), T-junction was designed to generate droplets, where the side channel (50 μm in height and 80 μm in width) of T-junction was vertical to the main channel and thinner than it (100 μm in height). In the meanwhile, the width of main channel decreased to a half of the original one at T-junction to increase flow rate and enhance shear force here. The extracting reagent was injected into the side channel, while the aqueous sample solution was injected into the main channel (1000 μm in width). Then monodisperse droplets would rapidly generate and disperse in the aqueous sample solution flow. In liquid–liquid extraction part (Fig. 1b), a long main channel with suitable length was designed to provide enough time for liquid–liquid extraction. In our experiments, a straight channel was chosen to simplify the experiments for confirming the liquid–liquid extraction in our system. In droplets collection part (Fig. 1c), guiding tracks (functioned as a groove with a depth of 30 μm and width of 80 μm) were designed on the top surface of the main channel. The guiding tracks, which had an included angle of 15 degree to the flow direction, covered the width direction of the main channel. At the end of the guiding tracks (Fig. 1d), a connecting channel (100 μm in width, 100 μm in length and 100 μm in height) between the main channel and the collecting channel was designed to collect the absorbing reagent. An actual image of the microchip was shown in Fig. 1e and the image of the device placed under microscope was shown in Fig. 1f.

Modification of microchip

Surface of the microchannels on microchip was modified with poly(allylamine hydrochloride) (PAH, Alfa Aesar, USA) and poly(sodium 4-styrenesulfonate) (PSS, J&K, China) using reported layer-by-layer deposition method.[33] Firstly, microchip was treated by oxygen plasma and the surface of microchannels would become negative charged (Fig. S1a, ESI†). PAH solution (0.1% w/v PAH in 0.5 M NaCl solution) was injected into the microchannels, and then the microchip was incubated at room

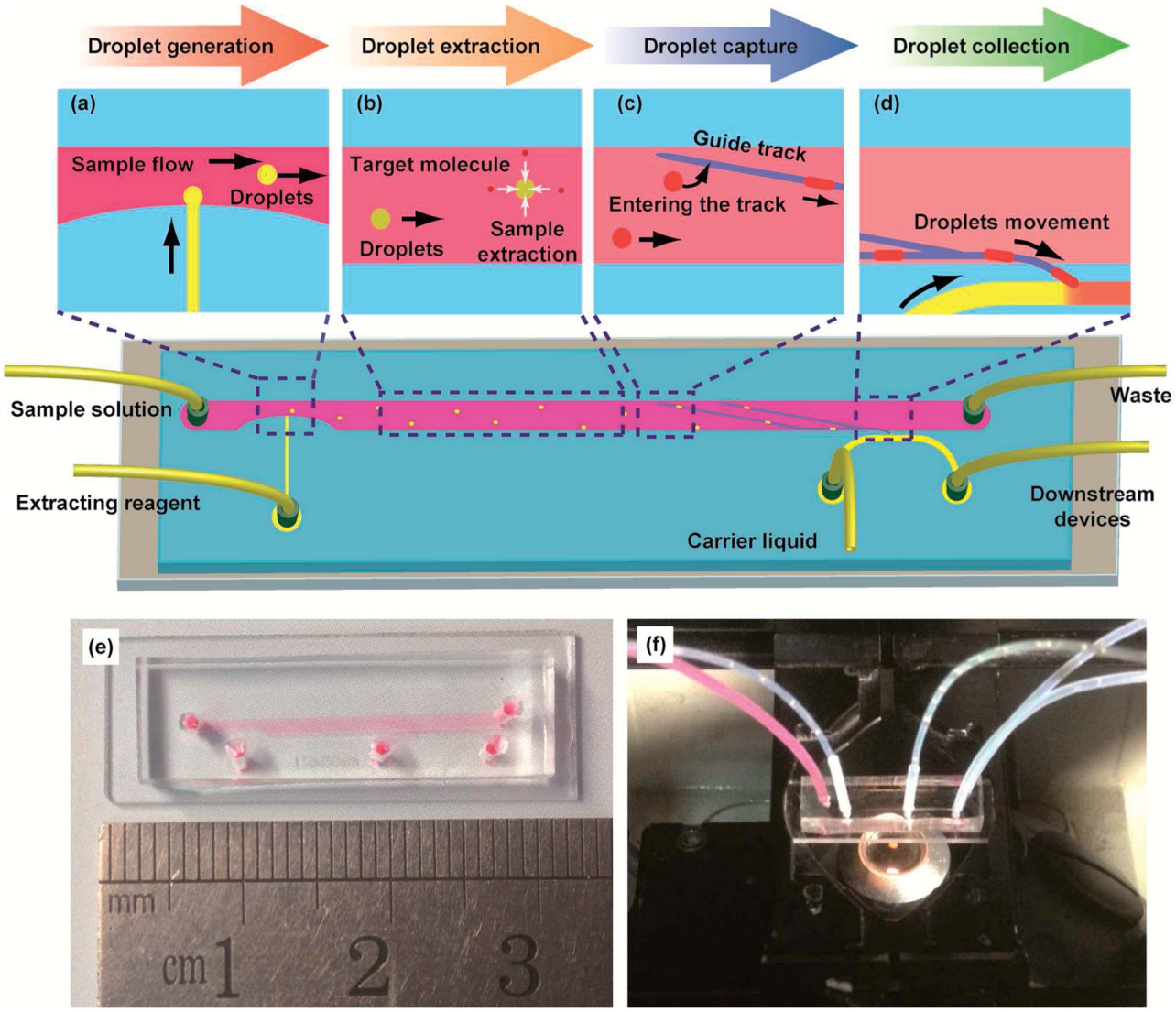

Fig. 1 Microfluidic device for monodisperse droplets liquid–liquid extraction. (a) Mechanism of the droplet generation part. Organic reagent and sample solution were injected into the side channel and the main channel respectively. (b) Mechanism of the liquid–liquid extraction part. Target molecules transferred into the organic droplets near the interface of the droplets and the sample flow. (c) Design of the guiding tracks. Droplets after extraction were led to one side of the channel. (d) Mechanism of the droplets collection part. Droplets were received by the connecting channel to the collection channel. (e) An image of the microchip filled with red dye. (f) An image of the actual device placed on the object stage of a fluorescence microscope.

temperature for 10 min. During that time, positive charged polyelectrolyte would be attracted by negative charge and deposited onto the surface of microchannels (Fig. S1b, ESI†). After washing with 0.1 M NaCl solution, the microchannels were filled with PSS solution (0.1% w/v PSS in 0.5 M NaCl solution) and incubated at room temperature for another 10 min to perform the deposition of PSS (Fig. S1d, ESI†). The microchannels were washed by 0.1 M NaCl solution again to remove unsteadily attracted PSS. Then PAH solution and PSS solution were repeatedly injected in turns using similar procedures to carry out another round of deposition. At last, three rounds of deposition were performed and the surface of microchannels was modified to be hydrophilic. The modification process of the microchips was detailed in ESI Fig. S1.†

Generation and collection of droplets

During all the experiments, microscope was used to monitor the generation and collection of monodisperse droplets. In the droplets generation part, water with red dye was injected into the main channel to simulate the sample solution, and butanol was injected into the side channel to act as the extracting reagent. To optimize the droplets generation, we applied different flow rates of sample solution and butanol to adjust the rates of droplets generation as well as the sizes of droplets. After the droplets based liquid–liquid extraction, the monodisperse droplets reached the droplets collection part. Finally, butanol was also injected into the collecting channel as the absorbing reagent to collect the droplets containing target molecules after online liquid–liquid extraction. To realize better collection of

droplets, we investigated the influences of the tilt angles and sizes of the connecting channel to improve the droplets collecting process.

Online monodisperse droplets based liquid–liquid extraction on the whole microchip

After the droplets of extracting reagent were generated, they would flow through liquid–liquid extraction part of the microchip and reach the droplets collection part. At the end of liquid–liquid extraction part, guiding tracks were designed to initiate the droplets collection and droplets were captured and guided by guiding tracks. Different from guiding tracks for plug-like droplets,[34] guiding tracks in our system mainly depended on the buoyancy to capture monodisperse droplets. To further indicate the successful liquid–liquid extraction of molecules in aqueous samples by monodisperse droplets in our microfluidic device, aqueous solution containing 10 μM fluorescein sodium was used as the continuous phase and the extraction of fluorescein sodium was studied. Briefly, aqueous solution containing 10 μM fluorescein sodium was injected into microchip through the inlet of main channel, and droplets of butanol were dispersed in it. Simultaneously, butanol was injected into the collecting channel to absorb the droplets coming from the guiding tracks. During this experiment, fluorescence microscope was also utilized to monitor the collection of droplets and record the results of extraction.

Results and discussion

Droplets generation on the microchip

To investigate the droplets generation, water with red dye was injected into the main channel at a flow rate of 5 μL min^{-1} to simulate the sample solution, and butanol was injected into the side channel at a flow rate of 0.1 μL min^{-1} to act as the extracting reagent. In order to confirm the generation of monodisperse droplets on this microchip, the injection of water containing red dye and butanol were performed simultaneously. Because of the height difference between side channel and main channel in this part (Fig. 2a), a spherical interface between butanol and aqueous solution was much easier to form and this kind of interface was helpful for the generation of monodisperse droplets. As shown in Fig. 2, monodisperse droplets were successfully generated in this system, more details were shown in Video 1.†

By adjusting the flow rate of sample solution and extracting reagent, both the droplets generating rate and the droplets size could be well controlled. In our experiments, appropriate rate of droplet generation as well as the size of droplets was optimized to meet the requirements for performing successful extraction and collection of droplets. The results showed that the droplets would not be effectively trapped in the guiding track when their size was too small. However, it would be difficult for them to pass through the narrow connecting channel when the droplets size was too big. As an influence of the droplets generating speed, it was obvious that the droplets suspended in the sample flow would be lacked when the speed is too low, resulting in low

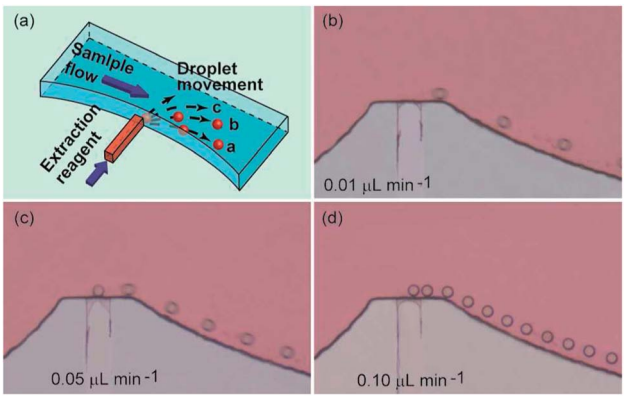

Fig. 2 Optimization of flow rate of the extracting reagent for the monodisperse droplets generation. (a) Schematic 3D structure of the droplet generating part and the schematic diagram for droplets generation. (b–d) Micrographs of droplets generation at different flow rates. Butanol was injected into the side channel at a rate of 0.01 μL min^{-1} (b), 0.05 μL min^{-1} (c), and 0.10 μL min^{-1} (d), respectively.

extraction efficiency. In the meantime, moving velocity of the droplets in the main channel would become slower when they entered the guiding tracks. Thus, a latter droplet would catch up with the former one when the droplets generating speed is too high, which caused those two droplets to fuse to be one bigger droplet. Under this situation, it might be difficult for the bigger droplet to pass through the connecting channel and enter the collecting channel. In order to simplify the optimization process, we selected the flow rate of the sample flow in the main channel as 5 μL min^{-1}. Then, we used different flow rates (0.01, 0.05, 0.1, 0.5 and 1.0 μL min^{-1}) (data at high flow rates were not shown) of the extracting reagent in the side channel to investigate the influence of the flow rate of the extracting reagent on the droplets generating speed. The results showed that droplets generating speed became higher and the diameter of droplets kept unchanged (about 40 μm) when the flow rate of the extracting reagent increased from 0.01 to 0.10 μL min^{-1} (Fig. 2). When flow rates of extracting reagent further increased (for example, 0.5 or 1.0 μL min^{-1}), bigger droplets (diameter was about 100 μm) would generate at a lower generating speed (as shown in droplets collection part). In the experiments with appropriate control, the droplets generated at the interchange of the main channel and the side channel could randomly enter into the sample flow at different directions, for example direction *a*, *b* and *c* (Fig. 2a), which detailed in Video 1.† As a result, the droplets suspended well in the sample flow well, which would raise the extraction efficiency. For further use of this microchip, speed of droplets generation and size of droplets should be adjusted according to the detailed requirement of the experiments.

Capture and collection of droplets

After online droplets based liquid–liquid extraction, guiding tracks (depth: 30 μm, width: 80 μm) on the top face of the channel were designed to guide the droplets to the collecting channel. As the chosen extracting reagent had a lower density

than that of the aqueous solution, buoyancy promoted the monodisperse droplets of extracting reagent to enter into the guiding tracks while droplets passed through those guiding tracks. Buoyancy also gave aid to the capture of droplets that already entered the guiding tracks. Monodisperse droplets in guiding tracks had to overcome the buoyancy to escape from the guiding tracks and pass through the guiding tracks, especially for the smaller ones (for example, droplets generated with a diameter of 40 μm) that were totally trapped into guiding tracks (Fig. S2a and b, ESI†). For bigger monodisperse droplets (diameter: about 100 μm) which were even a little wider than guiding tracks, surface tension also had a contribution to the capture of the droplets: surface tension made the droplets keep spherical and prevented them from leaving the guiding tracks by changing their shapes (Fig. S2c and d, ESI†). As a result, these droplets were trapped in guiding tracks and moved along the tracks. At last, droplets in guiding tracks would be led to the connecting channel between main channel and collecting channel. In later experiments, droplets with a diameter of about 100 μm which were a litter bigger than guiding tracks were applied and studied.

Appropriate width and tilt angle of connecting channel was important for droplets collection, because they would influence the flow velocity in connecting channel. Very low flow velocity in connecting channel might lead to the failure of droplets collection, while very high flow velocity in connecting channel would allow sample solution in main channel to pass through the connecting channel and entered the collecting channel. Then a software COMSOL multiphysics was used to simulate the velocity field near the connecting channel to achieve better collection of monodisperse droplets that came from the guiding tracks. The length and width of connecting channel and its tilt angle with the main channel were optimized using this software. The results showed that the length and width of connecting channel had a greater influence on the function of connection than the tilt angle did (Fig. 3). The flow velocity in the connecting channel became lower when the length of the connecting channel obviously increased (Fig. 3a), while it became higher when the width of the connecting channel increased (Fig. 3b). For the designs with different tilt angles between the connecting channel and the main channel, only the ones with tilt angles smaller than 45 degree or bigger than 135 degree had significantly different results (Fig. 3c).

According to the simulation above, microchips with different designs of connecting channel were fabricated and tested in the experiments for droplets collection, and the results of actual experiments were consistent with the simulation results. Based on the results, connecting channel with a width of 100 μm, a length of 100 μm and a tilt angle of 150 degree was chosen for further usage in following experiments. Under the optimized conditions, we investigated droplets capture and collection using water with red dye as the sample solution and butanol as the extracting reagent. When the monodisperse droplets reached the guiding tracks, they were successfully captured and moved along the guiding tracks (Fig. 4a–d). Finally, they passed through the connecting channels, entered the collecting channel and were successfully collected (Fig. 4e and f). More details about the capture and collection of droplets were shown in Video 2.†

Online monodisperse droplets based liquid–liquid extraction on the whole microfluidic device

According to the experiments where water containing red dye was used as the aqueous sample solution and butanol as the extracting reagent, we demonstrated that the established microfluidic device could successfully perform monodisperse droplets generation, liquid–liquid extraction and droplets collection. Both generation rate and size of the monodisperse droplets could be adjusted to meet the requirement for online liquid–liquid extraction and the collection of droplets. We had optimized the flow rates in the side channel and the design of the connecting channel. In the following experiments, the flow rate of the main channel and the side channel were selected as 5 μL min^{-1} and 0.5 μL min^{-1} respectively. According to the optimization and corresponding experiments, the connecting channel (100 μm in length, 100 μm in width) with a tilt angle of 150 degree with the main channel was used in the following experiments.

To confirm the feasibility of online liquid–liquid extraction on the designed microchip, we studied the extraction of fluorescein sodium in water by butanol droplets. A real sample (water containing 10 μM fluorescein sodium) was injected into the main channel at a flow rate of 5 μL min^{-1}, while organic extracting reagent (butanol) was injected into the side channel at a flow rate of 0.5 μL min^{-1} in the droplets generation part. Then the monodisperse droplets of butanol with a diameter of about 100 μm would disperse in the real sample solution flow and move forward with the sample flow. After that, the butanol droplets reached the droplets collection part in about 30 s, during which time fluorescein sodium in water could be extracted into the butanol droplets. The fluorescence images observed by fluorescence microscope indicated that fluorescence intensities of the droplets became stronger while the monodisperse droplets were moving forward with the real sample solution flow (Fig. 5–c), which indicated that the fluorescein sodium was successfully extracted into the organic droplets. The fluorescent intensities of the droplets at different positions were calculated by QCapture Pro software (Version 5.1.1.14, Media Cybernetics, USA). As shown in Fig. 5d, the fluorescence intensities of the droplet increased significantly as the droplets moved away from the droplets generation part, indicating that extracting efficiency would be visibly raised when we lengthened the extraction channel which provided a longer time for extraction. Even though complete distribution equilibrium was not achieved, the current extracting efficiency after a rapid extraction in chips was enough for detection and online monitor. In the meantime, elongation of the extracting channel of this microchip was proved to be a feasible way to increase the extracting efficiency if necessary. Applying smaller droplets or lower flow rate of sample solution was also believed to be helpful for the complete distribution equilibrium. Based on these results, the length of extracting channel was set to 15 mm in this work unless special explanation was mentioned.

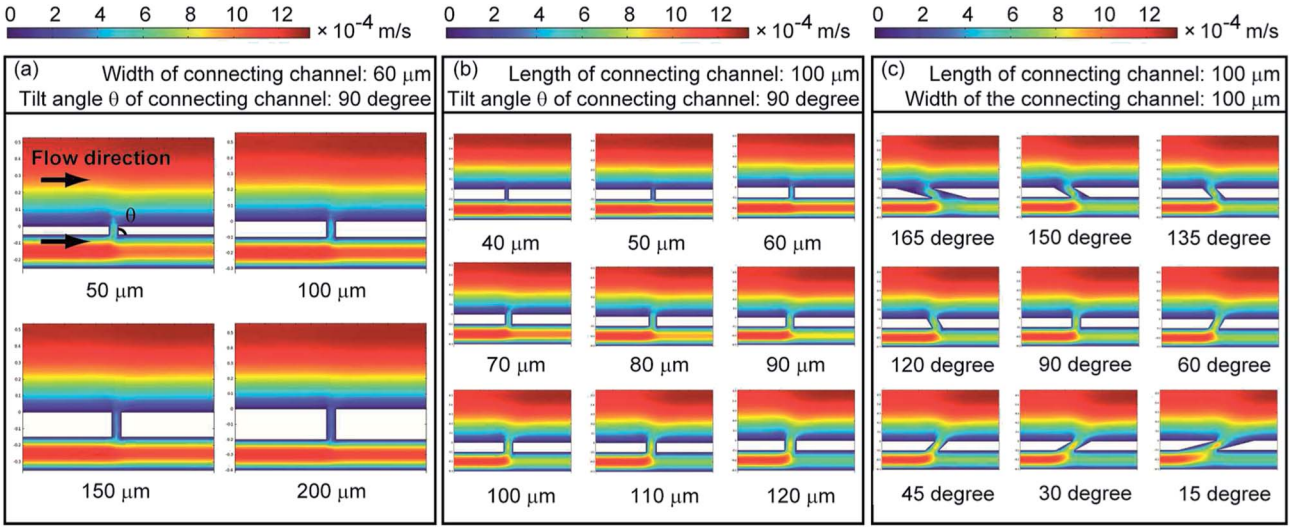

Fig. 3 Simulation of the flow velocity field near connecting channel. (a) Influences of the length of the connecting channel. The width of the connecting channel was set as 60 μm, and the tilt angle of connecting channels was set as 90 degree. (b) Influences of the width of the connecting channel. The length of the connecting channel was set as 100 μm, and the tilt angle of connecting channels was set as 90 degree. (c) Influences of the tilt angle of the connecting channel. The length of the connecting channel was set as 100 μm, and the width of connecting channels was set as 100 μm.

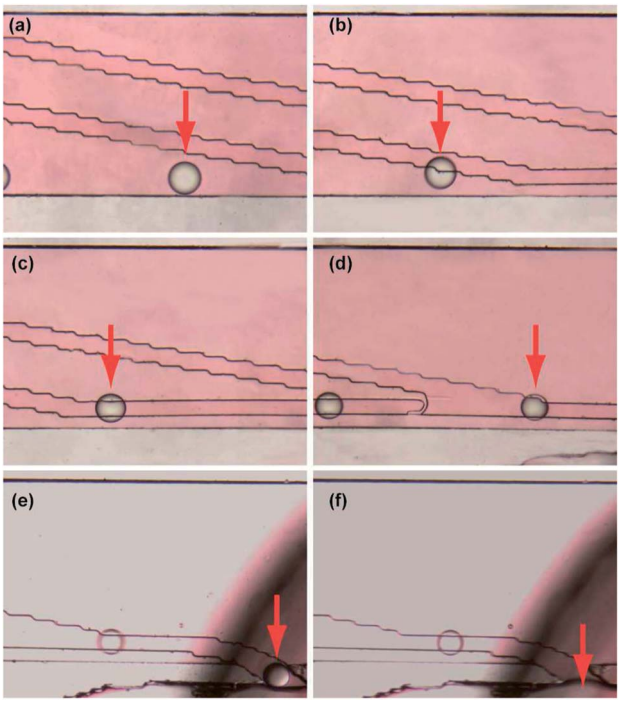

Fig. 4 Capture in guiding track and collection of the droplets. (a–d) Droplet entered the guiding track and moved along the track. (e and f) Droplet passed through the connecting channel to the collecting channel and was absorbed by absorbing solution. Red arrows were used to mark the moving droplet.

When these droplets of butanol reached the droplets collection part, they would enter the guiding tracks and move along the tracks as discussed before. Finally, these monodisperse droplets passed through the connecting channel and then were absorbed by absorbing reagent (butanol was used here) in collecting channel (Fig. S3b and c, ESI†). When these droplets were absorbed into the non-fluorescent organic extracting reagent, different fluorescent intensities

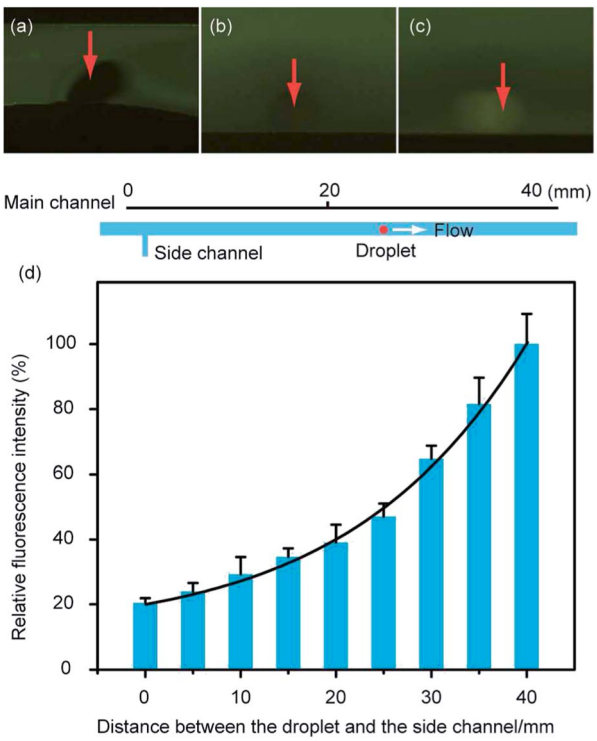

Fig. 5 Online monodisperse droplets based liquid–liquid extraction of fluorescein sodium. (a) Fluorescence image of the droplet when it was just generated. (b) Fluorescence image of the droplet when it flowed over a distance of 20 mm away from its generation position. (c) Fluorescence image of the droplet when it flowed over a distance of 40 mm away from its generation position. (d) Increasing fluorescence intensities of the droplet when it passed through the main channel.

of the mixture of absorbing reagent and organic droplets were obviously observed (Fig. S3b and c, ESI†). By adjusting the flow rates in collecting channel and the generation rate of droplets, several droplets could be absorbed and detected together to provide a stronger signal, which would enhance the detection sensitivity. However, real sample solution would flow into the connecting channel and even the collection channel, if the flow rate in the collecting channel was too low ($\leq$0.5 μL min^{-1}) (Fig. S3a, ESI†). Instead, absorbing reagent would flow into the connecting channel if the flow rate in the collecting channel was too high ($\geq$4 μL min^{-1}), which would prevent the droplets from passing through the connecting channel to the collecting channel (Fig. S3d, ESI†). Each of the two cases could result in the failure of droplets collection. The fluorescence intensities of absorbing solution flow in the collection channel were calculated by Qcapture Pro software, and the results were shown in ESI Fig. S3e.† The results showed us that the fluorescence intensities of the absorbing solution increased when the flow rates of the absorbing solution were slowed down. Thus, the flow rate of the extracting reagent was set as 1 μL min^{-1}.

All the results indicated that online monodisperse droplets based liquid–liquid extraction of fluorescein sodium was well performed on the microfluidic chip. After droplets generation in the first part, they dispersed in the real sample flow in the main channel and extraction successfully carried out in the main channel. The organic droplets containing extracted fluorescein sodium were collected and observed by an inverted fluorescence microscope. Therefore, the established microfluidic device was believed to be a useful tool for online sample pretreatment.

Conclusion

In summary, an integrated microfluidic device for online monodisperse droplets based liquid–liquid extraction was established and demonstrated by the online extraction of fluorescein sodium. The monodisperse droplets well extracted fluorescein sodium, and the droplets were successfully collected by the absorbing reagent in the collecting channel. Contrast to the reported methods on droplet-based extraction on microchip,[25,26,28] aqueous solution and organic monodisperse droplets were separated by an online process in our system and complex accessorial components of the chip, such as integrated electrodes were avoided to manipulate the droplets. We believed the established microfluidic device was a useful tool for online droplet-based extraction. Because there was no special requirements for the extracting reagents and sample solution, it was convenient to replace the butanol with other extracting reagents for better extraction of compounds that chemists were interested in. As the monodisperse droplets in the liquid–liquid extracting part of this microchip were continuously renewed, the method had the potential for time-resolved monitoring. Moreover, the microdevice could be easily connected to downstream devices for further analysis, such as mass spectrometer and liquid chromatography.

Acknowledgements

This work was supported by National Natural Science Foundation of China (nos 21227006 and 91213305).

Notes and references

1 G. Velve-Casquillas, M. Le Berre, M. Piel and P. T. Tran, *Nano Today*, 2010, **5**, 28–47.
2 T. Chován and A. Guttman, *Trends Biotechnol.*, 2002, **20**, 116–122.
3 P. Yager, T. Edwards, E. Fu, K. Helton, K. Nelson, M. R. Tam and B. H. Weigl, *Nature*, 2006, **442**, 412–418.
4 K. F. Jensen, J. El-Ali and P. K. Sorger, *Nature*, 2006, **442**, 403–411.
5 W.-Y. Lin, Y. Wang, S. Wang and H.-R. Tseng, *Nano Today*, 2009, **4**, 470–481.
6 P. W. Miller, L. E. Jennings, A. J. deMello, A. D. Gee, N. J. Long and R. Vilar, *Adv. Synth. Catal.*, 2009, **351**, 3260–3268.
7 Y. Wang, C. Phillips, W. Xu, J. H. Pai, R. Dhopeshwarkar, C. E. Sims and N. Allbritton, *Lab Chip*, 2010, **10**, 2917–2924.
8 J. Voldman, A. M. Skelley, O. Kirak, H. Suh and R. Jaenisch, *Nat. Methods*, 2009, **6**, 147–152.
9 T. Liu, B. Lin and J. Qin, *Lab Chip*, 2010, **10**, 1671–1677.
10 R. Hu, X. Feng, P. Chen, M. Fu, H. Chen, L. Guo and B. F. Liu, *J. Chromatogr., A*, 2011, **1218**, 171–177.
11 S. Wu, Y. Zhang, H. Shen, B. Su and Q. Fang, *Chem. Commun.*, 2011, **47**, 5723–5725.
12 Y. Zhu, H. Chen, G. Du and Q. Fang, *Lab Chip*, 2012, **12**, 4350–4354.
13 H. S. Moon, K. Kwon, S. I. Kim, H. Han, J. Sohn, S. Lee and H. I. Jung, *Lab Chip*, 2011, **11**, 1118–1125.
14 H. Wei, B. Chueh, H. Wu, E. W. Hall, C. Li, R. Schirhagl, J.-M. Lin and R. N. Zare, *Lab Chip*, 2010, **11**, 238–245.
15 W. Liu, H. Wei, Z. Lin, S. Mao and J.-M. Lin, *Biosens. Bioelectron.*, 2011, **28**, 438–442.
16 Y. Wan, Y. Liu, P. B. Allen, W. Asghar, M. A. I. Mahmood, J. Tan, H. Duhon, Y. Kim, A. Ellington and S. M. Iqbal, *Lab Chip*, 2012, **12**, 4693–4701.
17 K. Vijayakumar, S. Gulati and J. B. Edel, *Chem. Sci.*, 2010, **1**, 447–452.
18 P. Liu, X. Li, S. A. Greenspoon, J. R. Scherer and R. A. Mathies, *Lab Chip*, 2011, **11**, 1041–1048.
19 H. Wei, H. Li, S. Mao and J.-M. Lin, *Anal. Chem.*, 2011, **83**, 9306–9313.
20 D. Gao, H. B. Wei, G. S. Guo and J.-M. Lin, *Anal. Chem.*, 2010, **82**, 5679–5685.
21 H. Yang, J. M. Mudrik, M. J. Jebrail and A. R. Wheeler, *Anal. Chem.*, 2011, **83**, 3824–3830.
22 K. A. Hagan, W. L. Meier, J. P. Ferrance and J. P. Landers, *Anal. Chem.*, 2009, **81**, 5249–5256.
23 E. Z. Lee, Y. S. Huh, Y.-S. Jun, H. J. Won, Y. K. Hong, T. J. Park, S. Y. Lee and W. H. Hong, *J. Chromatogr., A*, 2008, **1187**, 11–17.
24 M. D. R. Payán, H. Jensen, N. J. Petersen, S. H. Hansen and S. Pedersen-Bjergaard, *Anal. Chim. Acta*, 2012, **735**, 46–53.

25 Y. H. Choi, Y. S. Song and D. H. Kim, *J. Chromatogr., A*, 2010, **1217**, 3723–3728.
26 P. Mary, V. Studer and P. Tabeling, *Anal. Chem.*, 2008, **80**, 2680–2687.
27 J. G. Kralj, H. R. Sahoo and K. F. Jensen, *Lab Chip*, 2007, **7**, 256–263.
28 H. Chen, Q. Fang, X. F. Yin and Z. L. Fang, *Lab Chip*, 2005, **5**, 719–725.
29 M. C. Morales and J. D. Zahn, *Microfluid. Nanofluid.*, 2010, **9**, 1041–1049.
30 H. Shen and Q. Fang, *Talanta*, 2008, **77**, 269–272.
31 H. Lee, L. Xu, B. Ahn, K. Lee and K. W. Oh, *Microfluid. Nanofluid.*, 2012, **13**, 613–623.
32 V. van Steijn, C. R. Kleijn and M. T. Kreutzer, *Lab Chip*, 2010, **10**, 2513–2518.
33 W. A. C. Bauer, M. Fischlechner, C. Abell and W. T. S. Huck, *Lab Chip*, 2010, **10**, 1814–1819.
34 J. Xu, B. Ahn, H. Lee, L. Xu, K. Lee, R. Panchapakesan and K. W. Oh, *Lab Chip*, 2012, **12**, 725–730.
35 K. Zhang, Q. Liang, S. Ma, T. He, X. Ai, P. Hu, Y. Wang and G. Luo, *Microfluid. Nanofluid.*, 2010, **9**, 995–1001.
36 T. Bowman, J. Frechette and G. Drazer, *Lab Chip*, 2012, **12**, 2903–2908.
37 Y. Zhu and Q. Fang, *Anal. Chem.*, 2010, **82**, 8361–8366.
38 P. A. Romero and A. R. Abate, *Lab Chip*, 2012, **12**, 5130–5132.
39 Y.-Y. Chen, Z.-M. Chen and H.-Y. Wang, *Lab Chip*, 2012, **12**, 4569–4575.
40 S. Y. Jung, S. T. Retterer and C. P. Collier, *Lab Chip*, 2010, **10**, 2688–2694.
41 Y. Xia and G. M. Whitesides, *Annu. Rev. Mater. Sci.*, 1998, **28**, 153–184.

